

Dear reviewer,

The reviewer's comments were highly insightful and enabled us to improve the quality of our manuscript. Our point by point responses to the each of the comments in the following pages. We hope that the revisions in the manuscript and our accompanying responses will be sufficient to make our manuscript suitable for publication in *Atmospheric Measurement Technique*.

Changes to the revised manuscript are shown in red.

10 We shall look forward to hearing from you at your earliest convenience.

Yours sincerely,

Professor Yong-Jun, Kim.

15

Address: School of Mechanical Engineering, Yonsei University, Seoul, Korea

Phone: +82-2-2123-7212

Fax: +82-2-312-2159

E-mail: yjk@yonsei.ac.kr

20

OPEN DISCUSSION #2

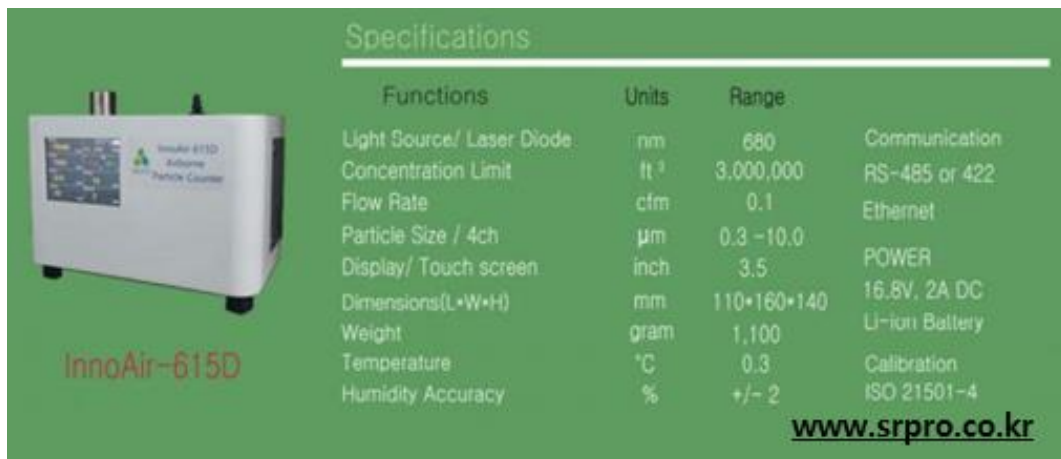
Question 1

No information is provided about the detector, which is a key component of the instrument, so I can only guess what it is. My suspicion is that this is one of the class of optical dust sensors that have been used as PM2.5 surrogate sensors. Such a sensor might yield quantitative data in this application, if the performance could be demonstrated to be stable over time.

Answer 1

We thank for your advice. Although the main argument of the manuscript is the chip-sized particle growth chip, there is little information about the detector.

The optical detector used in the proposed system is a detection part of the commercial optical particle counter (Innoair-615D, Innociple Co., KR) which is capable of counting individual particles larger than 0.3 μm (Fig. R1).



Functions	Units	Range	
Light Source/ Laser Diode	nm	680	Communication
Concentration Limit	ft ³	3,000,000	RS-485 or 422
Flow Rate	cfm	0.1	Ethernet
Particle Size / 4ch	μm	0.3 -10.0	POWER
Display/ Touch screen	inch	3.5	16.8V, 2A DC
Dimensions(L*W*H)	mm	110*160*140	Li-ion Battery
Weight	gram	1,100	Calibration
Temperature	$^{\circ}\text{C}$	0.3	ISO 21501-4
Humidity Accuracy	%	+/- 2	

www.srpro.co.kr

Figure R1: The specification of the commercial optical particle counter. Its detection part was used in this study.

Figure R2 shows the (a) exploded view, (b) section A-A' and (c) section B-B' of the optical detector. It consists of the sensing chamber and optics (laser, cylindrical lens, elliptic mirror, optical detector, light trap). Introduced droplets are firstly arranged in a row in the acceleration nozzle (i.e., the outlet of the particle growth chip) and enter the sensing chamber. The droplets then pass through the place where the condensed thin beam is irradiated. The mirror collects the scattered light from a droplet and redirect it to the optical detector.

When the laser beam passes through the cylindrical lens, the shape of the laser beam is not a point but a very thin surface. In addition, the acceleration nozzle at the chip outlet is only 0.8 mm in diameter and is located about 1.5 mm below the point where the beam passes. Therefore, as shown in Figure R2 (c), on the condition that the coincidence error does not occur (when two particles do not pass through the viewing volume at the same time), almost all the grown micro-droplets are counted in the optical detector.

In the perspectives of the structure and detection principle, the optical detector used in this study is similar to the high-precision OPC rather than dust sensors. Thus the proposed system demonstrated particle counting performance, which was comparable to those of the reference CPC (model 3772, TSI Inc., USA).

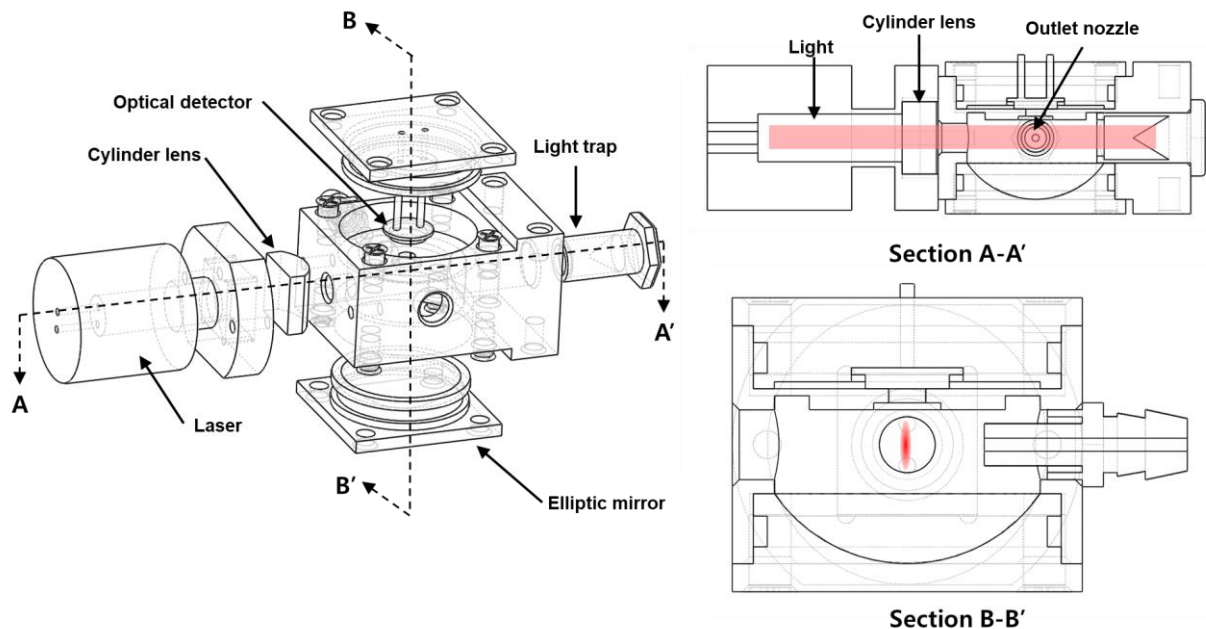


Figure R2: The (a) exploded view, (b) section A-A' and (c) section B-B' of the optical detector used in this study

We added the description of the optical detector in '2 Description of the MEMS-based CPC' of the revised manuscript as following,

~. The maximum Reynolds number in the channel at the given flow rate was only 32, which means that the sample stream in the channel was in the fully laminar regime.

The detection part of the commercial optical particle counter (OPC; Innoair-615D, Innociple Co., KR), which provided the time resolution of 6 s, was used as the optical detector in our system. It consists of the sensing chamber and optics (laser, cylindrical lens, elliptic mirror, optical detector, light trap). Introduced droplets are firstly arranged in a row in the acceleration nozzle (i.e., the outlet of the particle growth chip) and enter the sensing chamber. The droplets then pass through the place where the condensed thin beam is irradiated. The mirror directs the scattered light of a droplet to the sensing surface of the optical detector. When the laser beam passes through the cylindrical lens, the shape of the laser beam is not a point but a very thin surface. In addition, the acceleration nozzle at the chip outlet is only 0.8 mm in diameter and is located about 1.5 mm below the point where the beam passes. Therefore, on the condition that the coincidence error does not occur (the two particles do not pass through the viewing volume at the same time), almost all the grown micro-droplets are counted in the optical detector.

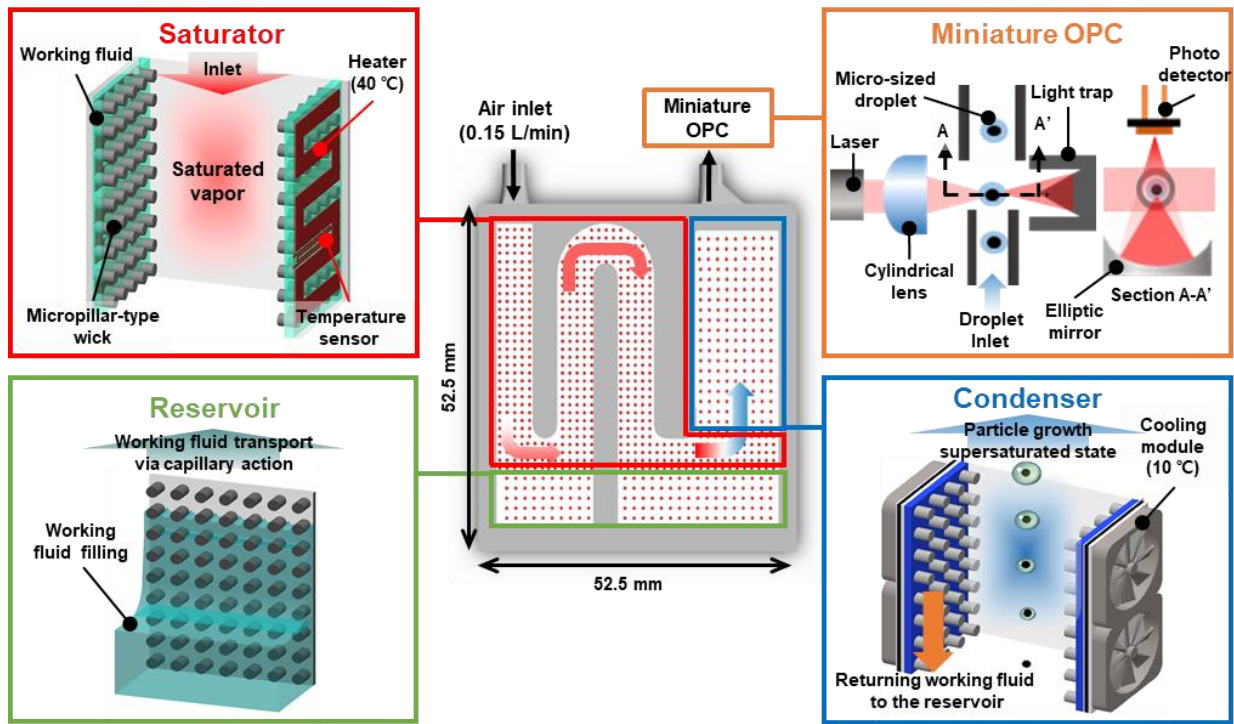
Question 2

I note that the sketch in Fig. 1 shows a more elaborate OPC design than in the simple optical detectors about which I have read or with which I have worked. Moreover, it shows a forward scattering instrument, but does not show a beam dump that is required for this geometry, suggesting that the cartoon does not represent the actual instrument.

Answer 2

We thank for letting us catch a mistake. We modified the schematic diagram of the miniature OPC based on the aforementioned mechanism in Answer 1.

We modified the schematic diagram of the miniature OPC in ‘Figure 1’ of the revised manuscript as following.



5

Figure 1: Schematic illustration of the MEMS-based CPC. The proposed system consists of four parts: the reservoir, saturator, condenser, and miniature OPC. The reservoir supplies the working fluid to the saturator via capillary action by the micropillar-type wick. The saturator heats the working fluid to generate saturated vapor. The saturated air becomes supersaturated when cooled by the condenser. UFPs grow into micro-sized droplets in the condenser and are counted by the miniature OPC.

10

Question 3

I further note that no mention is made of the pump employed, or the approach used for quantitative flow control. The instrument should be documented fully.

Answer 3

15

We thank for your advice and letting us improve the solidity of the manuscript. The MEMS-based CPC employed a micro pump (model 00H220H024, Nidec Co., JP) and a flow sensor (model FS1012-1020-NG, IDT Co., USA) for quantitative control. Furthermore, a lab-made circuit was used to regulate the flow rate based on the PID feed-back control. Moreover, we have described the customized circuit more clearly.

20

We added the description of the flow control and customized circuit in the ‘2 Description of the MEMS-based CPC’ of the revised manuscript as following.

Figure 2a shows our system with the customized circuit. The circuit, whose dimension is 90 mm x 65 mm, simultaneously reads the data from the miniature OPC, temperature sensor and flow sensor (model FS1012-1020-NG, IDT Co., USA), and controls the power of the heaters, cooling modules and micro pump (model 00H220H024, Nidec

Co., JP) via a pulse-width-modulation (PWM) method. In order for our system to be a stand-alone device, the feedback loops based on the proportional-integral-differential (PID) algorithm is implemented in the micro control unit (MCU) of the circuit, and their gains can be easily controlled using serial communication.

5 **We added the optical photograph of the customized circuit as Figure 2a in the revised manuscript as followings.**

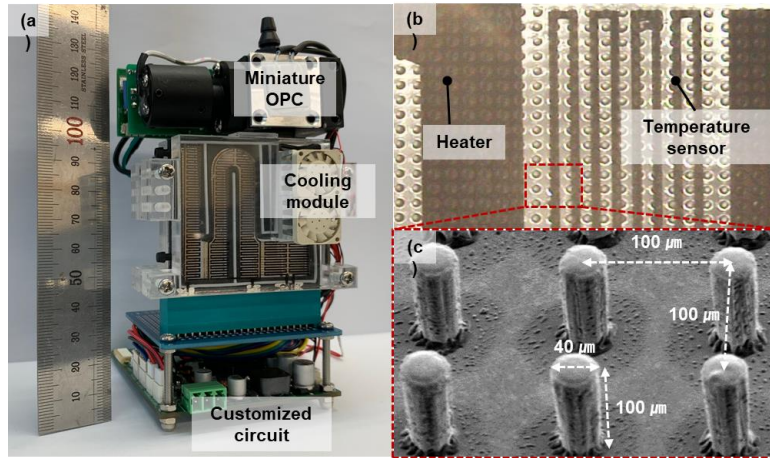


Figure 2: (a) Optical image of the proposed system; (b) magnified image of the heaters, resistive temperature sensors, and wick on the glass slide; and (c) scanning electron microscope (SEM) image of the micropillar-type wick.

10 **Question 4**

I further note that the authors have not identified the working fluid employed in their CPC.

Answer 4

We thank for letting us catch the mistakes in our manuscript. The kind of working fluid should be clearly stated in manuscript. We used Butanol as the working fluid of MEMS-based CPC.

15

We modified ‘Description of the MEMS-based CPC’ part of the revised manuscript as following.

Figure 1 shows the operating principle of the proposed MEMS-based CPC, which consists of a reservoir, saturator, condenser, and miniature OPC. To generate supersaturated vapor and hence grow UFPs to micro-sized droplets, the proposed system utilizes a conductive cooling method. Butanol was used as working fluid. The saturator generates saturated vapor by heating the wetted wall with the working fluid.

20

Question 5

The authors note that the CPC grows particles into 3.16 μm droplets, but provide no hint as to how they have determined this size. The instrumentation that they report is incapable of directly measuring particles of this size. I suspect that they have made the inference from the scattered light intensity detected by their OPC, but OPC measurements in this size range are highly uncertain owing to Mie resonances. A precision of 3 significant figures is highly unlikely.

25

Answer 5

A miniaturized OPC (PSM-615D, Innociple, KR) was used to characterize the counting performance of the proposed system, whereas another type OPC (OPC-N2, Alphasense, UK) was used to measure the mean diameters of the grown droplets. Both the OPCs are commercially available. The reason for using two kinds of OPCs is that, although the model PSM-615D can count a single droplet, it was not calibrated in terms of particle size. The model OPC-N2 is capable of not only measuring particles from 0.4 to 17 μm , but also having similar performance to the reference OPC (PAS-1.108, Grimm Technologies) (Sousan et al., 2016).

We modified the manuscript to clearly specify the measurement route for characterizing droplet size distribution, and refer to the measurement uncertainty induced by the Mie resonance. Also, the digit number of the droplet diameter was decreased to 2.

We further performed to characterize the mean diameter of the grown droplets when Ag particles in the size range from 20 to 140 nm were introduced, and move the results from the supplemental material to the result section in the revised manuscript.

We have added ‘5.1 Droplet size distribution’ in the result of the revised manuscript as following.

Figure 6 shows the size distribution of the droplets generated from the MEMS-based particle growth system. Monodisperse Ag particles in the size range from 20 to 140 nm were used as test aerosol and their number concentrations were fixed at around 2000 N cm^{-3} by adjusting the valves of the dilution bridge. The sampling time for measuring each droplet distribution was 2 min, and the corresponding measurement uncertainty based on the Poisson statistics was 0.13 %. All the error bars at each data point represent the standard deviations. The commercial OPC (OPC-N2, Alphasense, UK) was used for measuring the droplet size distribution. It was reported that OPC-N2 was capable of not only measuring particles from 0.4 to 17 μm , but also having moderate counting performance compared to the reference OPC (PAS-1.108, Grimm Technologies) (Sousan et al., 2016). The measurement errors induced from the Mie resonance was not considered in this data. The average droplet diameter ($d_{d,avg}$) was 3.1 μm when particles with the size of 20 nm, slightly larger than the minimum detectable size (12.9 nm), were introduced. Since the lower detectable size of the optical detector in the proposed system was 0.3 μm , introduced particles successfully grew into micrometer-sized droplets which were large enough to be counted by optical means. It was noted that the mean droplet size did not vary significantly above 40 nm. Also, most of the grown droplets were smaller than 10 μm , indicating that tens of micrometer-sized droplets, which could be attached to the inner walls of the particle growth system or optical detector via sedimentation, were barely generated.

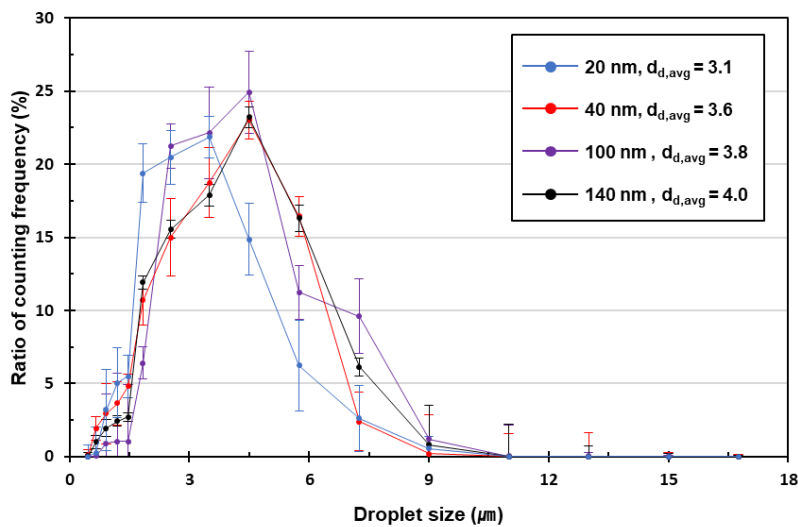


Figure 6: The size distribution of the droplets grown from the MEMS-based particle growth system when Ag particles of specific sizes were introduced.

We have added the reference which refers to the performance of OPC-N2 used in this study for measuring droplet size distribution in the revised manuscript.

Sousan, S., Koehler, K., Hallett, L., and Peters, T. M.: Evaluation of the Alphasense Optical Particle Counter (OPC-N2) and the Grimm Portable Aerosol Spectrometer (PAS-1.108), *Aerosol Sci Technol*, 50, 1352-1365, 2016

5

Question 6

The precision reported for accuracy of counts also seems excessive. A claim is made that the concentration accuracy is 4.1%, and later that it agrees with a reference CPC within 91.5%, suggesting double the uncertainty.

Answer 6

10 We thank for your advice and letting us modifying the ambiguous part. The value of 91.5 % reported in the conclusion of the manuscript represents that the difference in physical volume of the proposed system and commercial portable CPC (model 3007, TSI Inc., USA).

15 **Avoiding the ambiguity of this value, we have modified the related sentence in ‘6 Conclusion’ of the revised manuscript as following.**

Therefore, we modified the sentence. In terms of compactness and cost-efficiency, the proposed system is superior to conventional instruments. The physical volume of our system is only 8.5 % of the volume of the commercially-available portable CPC (e.g., model 3007, TSI Inc., USA).

20 Question 7

The orientation of the instrument also needs to be specified, as well as its sensitivity to orientation. I suspect that it must be operated with the saturator oriented vertically, with the reservoir at the bottom. What is the sensitivity to motion or tilting, as this is likely with a small, highly portable instrument? Also, if the optics are protected from flooding with working fluid, that would be of interest in ascertaining the instrument’s suitability for different applications.

25 Answer 7

In order to minimize the loss of droplets in the condenser via sedimentation, it is recommended that the MEMS-based CPC be oriented perpendicular to the surface. However, as advised by the reviewer, since the proposed system has been developed as a portable device for on-site monitoring of UFPs, its measurement performance should be evaluated when the device is tilted.

30 The design for preventing working fluid in the reservoir from flooding into the optics has not been done yet, which will be addressed in the future studies.

We have added the related experiment in ‘5.5 Performance comparison with the reference CPC’ of the revised manuscript as followings.

35 Figure 10 shows the measurement results of our system when it was tilted like an inset image. Monodisperse Ag particles with 25 nm were introduced and their concentrations were step-wisely increased from 0 to 4000 N cm⁻³. Since

the measurement was carried out for about 500 s at each angle, and the measurement uncertainty of each section was below 0.01 %. When the proposed system was oriented perpendicular to the surface, the counting efficiency of the proposed system was 2.04 % which was similar to the result of the size-dependent counting efficiency. When a 30 ° angle was applied, the counting efficiency was 7.07%. At 60°, the measurement difference compared to the reference CPC exceeded 10 % (16.3 %). Thus, it was found that, at a tilt angle of 60° or less, MEMS-based CPC can monitor UFPs without the significant degradation of the accuracy.

The deviation of the counting efficiency induced from applying a tilt angle can be explained by the sedimentation of droplets in the condenser. At 0 °, since the gravity direction was identical to the direction of the sample flow, the probability that grown droplets impacted on the condenser wall via sedimentation was negligible. However, with the increment of the tilt angle, the velocity vector of a droplet perpendicular to the channel increased, which lead to the decrement of the counting efficiency.

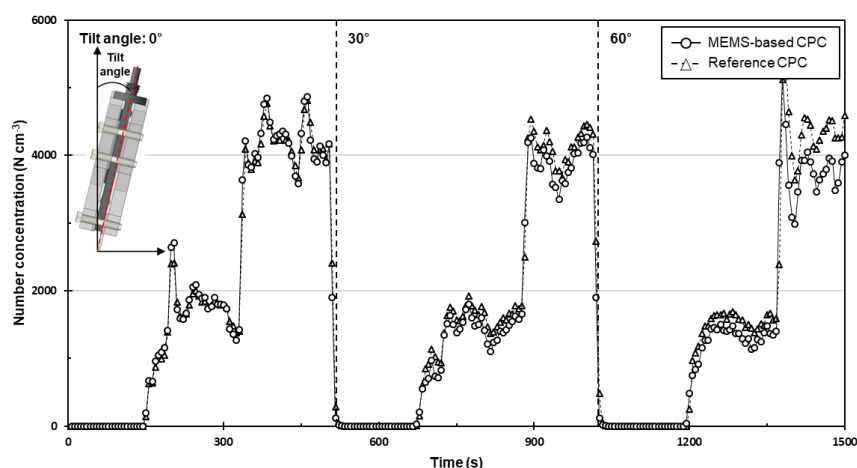


Figure 10: The time series of the number concentrations measured by the proposed system when it was tilted.

Question 8

The first paragraph of the introduction needs to be written with appropriate reference to the current understanding rather than that of two decades ago.

Answer 8

Thank you for your advice. We added recent references to the first paragraph of the introduction.

We modified ‘Introduction’ part of the revised manuscript as following,

Monitoring of airborne ultrafine particles (UFPs), which are smaller than 100 nm, is needed in various fields for human health and yield enhancement in industrial fields(Donaldson et al., 1998; Donovan et al., 1985; Hristozov and Malsch, 2009; Li et al., 2016; Liu et al., 2015). UFPs are mainly generated from burning fossil fuels and are ubiquitous in urban air; they account for about 90% of the total particle number concentration(Kim et al., 2011; Kittelson, 1998; Shi et al., 1999). Because of dramatic developments in nanotechnology, engineered UFPs for commercial and research purposes have been produced at a large scale. These incidentally and intentionally generated UFPs are more harmful to human health than larger counterparts: UFPs have a higher chance to deposit in the lower respiratory system and are more toxic owing to their larger surface-to-volume ratios, which causes oxidative stress, pulmonary inflammation, and tumor

development(Hesterberg et al., 2012; Hext, 1994; Li et al., 2003; Renwick et al., 2004). Thus, onsite monitoring is needed to assess and minimize UFP exposure. High-precision industries with cleanrooms also need UFP monitoring to increase the production yield. For instance, in the semiconductor industry, the minimum linewidth of the chips is approaching 7 nm(Neisser and Wurm, 2015). Particles that are a few nanometers in size are critical because “killer particles” (i.e., the diameter is greater than half of the minimum linewidth) can render the whole chip unusable(Libman et al., 2015). Unfortunately, since UFPs in cleanrooms are generated during fabrication processes (e.g., chemical vapor deposition (CVD), metallization, wet etching), contamination can occur in any manufacturing stages(Choi et al., 2015; Manodori and Benedetti, 2009). In these circumstances, a portable and low-cost sensor is needed for onsite UFP monitoring to accurately evaluate adverse health effects and control the contamination level in cleanrooms to enhance the production yield.

We have added the references in the 1st paragraph of the introduction in the revised manuscript.

(1) Li, N., Georas, S., Alexis, N., Fritz, P., Xia, T., Williams, M. A., Horner, E., and Nel, A.: A work group report on ultrafine particles (American Academy of Allergy, Asthma & Immunology): Why ambient ultrafine and engineered nanoparticles should receive special attention for possible adverse health outcomes in human subjects, *J Allergy Clin Immunol*, 138, 386-396, 2016.

(2) Liu, L., Urch, B., Poon, R., Szyszkowicz, M., Speck, M., Gold, D. R., Wheeler, A. J., Scott, J. A., Brook, J. R., Thorne, P. S., and Silverman, F. S.: Effects of ambient coarse, fine, and ultrafine particles and their biological constituents on systemic biomarkers: a controlled human exposure study, *Environ Health Perspect*, 123, 534-540, 2015.

(3) Kim, K. H., Sekiguchi, K., Kudo, S., and Sakamoto, K.: Characteristics of Atmospheric Elemental Carbon (Char and Soot) in Ultrafine and Fine Particles in a Roadside Environment, Japan, *Aerosol and Air Quality Research*, 11, 1-12, 2011.

(4) Hesterberg, T. W., Long, C. M., Bunn, W. B., Lapin, C. A., McClellan, R. O., and Valberg, P. A.: Health effects research and regulation of diesel exhaust: an historical overview focused on lung cancer risk, *Inhal Toxicol*, 24 Suppl 1, 1-45, 2012.

Question 9

The reference to clean room particle measurements is problematic because the flow rates through a miniature CPC will lead to poor counting statistics at the concentrations at which clean rooms operate.

Answer 9

You have raised an important point. Flow rate is an important factor that determines the quality of counting statistics in low concentration environment such as clean room.

Cleanrooms are classified according to the number and size of particles permitted per volume of air. In order to reduce the costs of the maintenance, the semiconductor industries separate one cleanroom facility into multiple classes; a cleanroom ranges from class 1 to class 100,000 depending on the processes taking place within the facility.

Clean rooms with class 1~10 require CPCs (e.g., Aerotrak^R 9001, TSI Inc., USA) with a high flow rate (2.83 LPM) to monitor the excessively low background concentrations. However, in cleanrooms with class 100 or 1000, the number concentration of background particles is in the order of 1 N cm^{-3} . In this case, although the proposed system operates at low volumetric flow rate ($0.15 \text{ LPM} = 2.5 \text{ cm}^3 \text{ s}^{-1}$), the measurement uncertainty based on the Poisson distribution reach 10 % in 40 s. Thus, it is expected that the proposed system can monitor the background concentration in cleanrooms with a satisfactory resolution. For example, Liao et al. also successfully measured the number concentration of backgrounds

(0.2 ~ 22.41 N cm⁻³) in a cleanroom using a portable CPC (model 3007, TSI Inc., USA) with a flow rate of 0.1 LPM (Liao et al., 2018).

We added a relevant discussion in the ‘5.4 Detectable concentration range’ of the revised manuscript as following.

Even if filtered air is introduced into a system, droplets may form in the condenser via homogeneous or ion-induced nucleation. Droplets without UFP nuclei cause false counting, which makes the system read a higher concentration than reality. This phenomenon is critical, especially in low-concentration environments. To evaluate the false counting of the proposed system, it was operated for 1 h with a HEPA filter connected to its inlet. When the temperature difference between the saturator and condenser was set to 30 °C, the average number concentration during the measurement period (background concentration) was only 0.05 N cm⁻³. This result indicated that homogeneous nucleation hardly occurred. Thus, the temperature profile was uniformly established inside the condensation chip because homogeneous nucleation typically occurs at low temperatures in regions where the local saturation ratio is high. **Owing to the low false count performance, our system can be applied to monitoring UFPs in cleanrooms with class 100 or 1000 whose background concentrations are in order of 1 N cm⁻³ (Liao et al., 2018). In these environment, the measurement uncertainty based on the Poisson statistics is expected to be 10 % in a sampling time of 40 s for a given flow rate (0.15 LPM = 2.5 cm³ s⁻¹).**

We have added the references in the ‘5.4 Detectable concentration range’ of the revised manuscript.

Liao, B.-X., Tseng, N.-C., Li, Z., Liu, Y., Chen, J.-K., and Tsai, C.-J.: Exposure assessment of process by-product nanoparticles released during the preventive maintenance of semiconductor fabrication facilities, *Journal of Nanoparticle Research*, 20, 2018.

Question 10

On p. 2, l. 13 reference is made to electrical techniques. I can only guess to what technology the authors are referring. If they wish to refer to a specific technology, they must define it in sufficient detail that the reader can understand it without having to trace through the literature citations that they give.

Answer 10

We thank for your advice and letting us improve the solidity of the manuscript. The electrical method in the manuscript is the particle detection method where the number concentration of UFPs is measured by electrically charging them and sensing their current. Following your suggestions,

We modified the ‘2nd paragraph of Introduction’ in the revised manuscript as following.

Condensation particle counters (CPCs) are one of the most widely used UFP detection instruments and are based on the heterogeneous particle condensation technique (Stolzenburg and McMurry, 1991). They grow UFPs to micro-sized droplets through condensation and capable of counting every single UFP by optical means. **Compared to an electrical method (measuring the number concentration of UFPs by electrically charging them and sensing their current), CPCs provide extremely sensitive and precise counting because they are capable of counting because they are capable of counting individual particles. (Kangasluoma et al., 2017; Kangasluoma et al., 2014; McMurry, 2000).**

Question 11

Error bars are needed on the data plots, and uncertainties on the quoted efficiencies. The uncertainties in the reported efficiencies need to take into account the Poisson counting statistics. The counting time is another piece of information that needs to be documented. It is quite reasonable to operate with a longer counting time than the TSI instrument with which they compare their data - as a trade-off in producing a much smaller instrument.

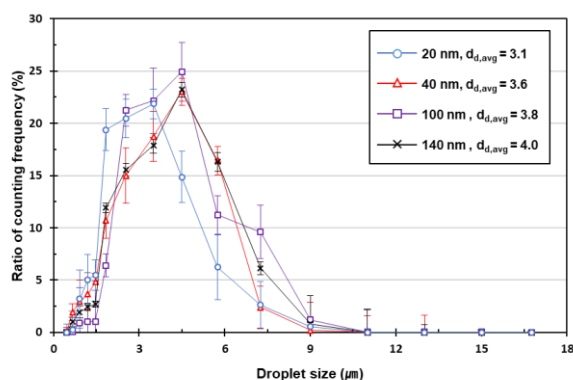
1. 35. The authors claim a lower detection limit on concentration of 8 particles/cm³. At the quoted flow rate, this concentration corresponds to about 20 counts/s. For a 1 s integrating time, this corresponds to a statistical (based on Poisson statistics) uncertainty of order 1/4. To claim uncertainty of 4%, a long count integration time is required. The authors need to be explicit about the parameters of the measurement, i.e., what is the integration/counting time?

Answer 11

The measurement uncertainties were specified in the results (droplet size distribution, size-dependent particle counting efficiency, detectable concentration range and performance comparison with the reference CPC) of the proposed system. Since the values of the uncertainty and standard errors were very small (in order of 0.1 %), the standard deviations were used as error bars for each result.

We have added the uncertainty in the '5.2 Droplet size distribution' of the revised manuscript.

Figure 6 shows the size distribution of the droplets generated from the MEMS-based particle growth system. Monodisperse Ag particles in the size range from 20 to 140 nm were used as test aerosol and their number concentrations were fixed at around 2000 N cm⁻³ by adjusting the valves of the dilution bridge. The sampling time for measuring each droplet distribution was 2 min, and the corresponding measurement uncertainty based on the Poisson statistics was 0.13 %. All the error bars at each data point represent the standard deviations.



25 Figure 6: The size distribution of grown droplets grown from the MEMS-based condensation chip when Ag particles of specific sizes were introduced.

We have added the uncertainty and error bars in the '5.3 Size-dependent particle counting efficiency' of the revised manuscript.

Figure 7 shows the size-dependent counting efficiency of the MEMS-based CPC. The size range of Ag particles was controlled concentration range to 1000-2000 N cm⁻³. The sampling times for each data point were 300 s, and the measurement uncertainty based on the Poisson statistics was 0.02%.

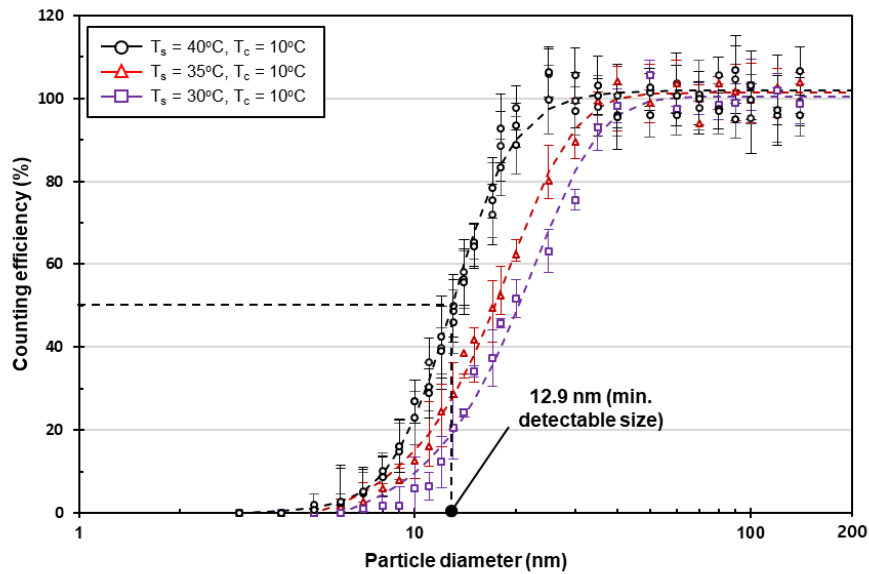


Figure 7: Particle counting efficiency of the MEMS-based CPC as a function of the particle size and saturator temperature. The particle size at which the particle counting efficiency was fitted to 50% was 12.9 nm ($T_s = 40^\circ\text{C}$), 17.3 ($T_s = 35^\circ\text{C}$) and 20.4 ($T_s = 30^\circ\text{C}$), respectively.

5

We have added the measurement uncertainty in the ‘5.5 Performance comparison with reference’ of the revised manuscript.

Figure 10 shows the measurement results of our system when it was tilted like an inset image. Monodisperse Ag particles with 25 nm were introduced and their concentrations were step-wisely increased from 0 to 4000 N cm^{-3} . Since the measurement was carried out for about 500 s at each angle, and the measurement uncertainty of each section was below 0.01 %.

10

We have added the measurement uncertainty in the 'Figure 9' of the revised manuscript.

	Diameter (nm)	28	26	24	22	20	18	16
Poisson statistics	Time interval (s)	96	66	84	72	108	108	66
	Uncertainty (%)	0.57	0.56	0.12	0.086	0.038	0.023	0.034
Number concentration (N cm ⁻³)	Reference CPC	8.36	18.99	223.84	585.87	1370.69	3733.96	4129.93
	MEMS-based CPC	7.99	17.65	224.58	619.10	1399.14	3809.45	4544.82
	Difference (%)	4.42	7.60	-0.32	-5.37	-2.03	-1.98	-9.12

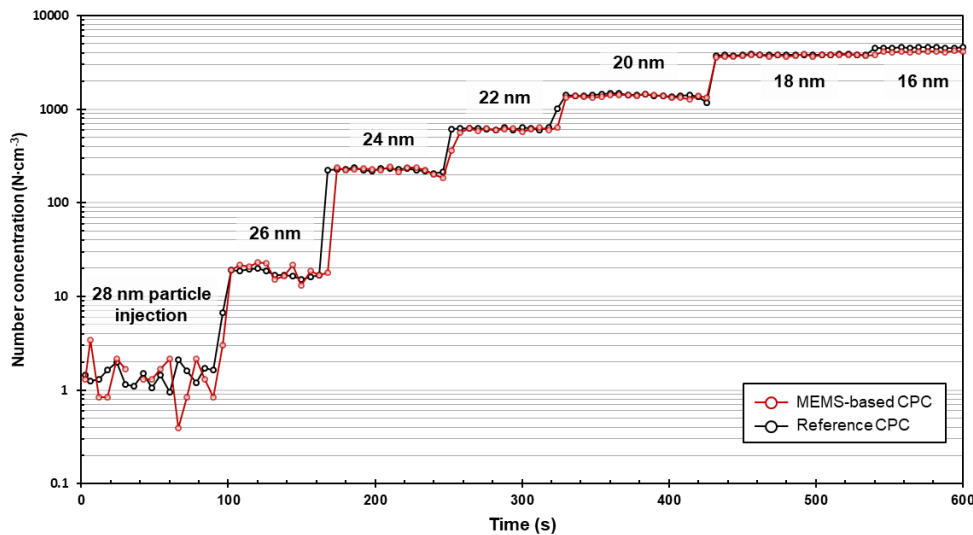


Figure 9: Time series of the number concentrations measured with the proposed system and reference CPC when the concentration and size were varied.

5 **Question 12**

On p. 3, l. 18, The authors note that a customized circuit was implemented for pulse-width-modulation. It would be highly desirable to document the nature of the control algorithm employed: is it P (proportional), PI (proportional-integral), or PID (proportional-integral-differential). Was the control algorithm implemented in software or in analog, hardware circuitry?

10 **Answer 13**

Please refer to Answer 3.

Question 13

p. 4: The experimental setup section describes the system in reasonable detail. It is unclear, how the quantitation was performed. The data presented in Fig 6 shows an asymptotic approach to 100% detection efficiency.

15

Were no large particles lost or otherwise not counted? Again, the nature of the optical detector and the way that the flow interfaces to it becomes an issue; How does the design ensure that all activated and grown particles pass through the view volume so that they can be counted. The analysis of the experimental results needs to clearly document all assumptions and approximations made in the data analysis. How were losses measured?

Fig. 6. The data shown reveal three groupings of data points, one below 10 nm, one 10-15 nm, and one for larger particles, but only up to 40 nm. What was changed for these data sets that show slight offsets and differences in noise levels? The calibration should be extended to larger particles since the tortuous path through the saturator could lead to losses, and the small dimensions might make those losses orientation dependent.

Answer 13

Because of the large difference between the flow rates of the commercial reference instrument and MEMS-based CPC, the following procedures were carried out to verify that particles with the same concentration were introduced into the two systems. First, to minimize the particle loss induced from the turbulence at the bifurcation, a flow splitter with a very small angle of cleavage (model 3708, TSI Inc., USA) was used. The tubes which leads to the both systems were electrostatic dissipative to minimize the electrostatic particle loss, and their lengths were carefully adjusted to match the transportation times.

To verify that the particles which introduced into both systems have the same concentrations, it was confirmed that the counting efficiency was close to 100 % when particles with size of 100 nm were introduced (it was assumed that they were activated and grew into droplets with 100 % efficiency). Then, while reducing the size of the introduced particles to 40 nm by adjusting the voltages of a DMA, it was confirmed whether the counting efficiency remained constant. Through these procedures, it was verified that the concentrations of the particles delivered to the two systems were the same.

The loss of the proposed system was characterized using the counting efficiency, since it is defined as the efficiency of the system at detecting the introduced particles, and thereby describes the overall transportation/activation efficiencies.

The size-dependent counting efficiency of the proposed system was further characterized using Ag particles in the size range of 3 to 140 nm (Figure 7). Particles with size of 140 nm were almost the maximum size that the Ag particle generator (EP-NGS20, EcoPictures, Co. KR) could generate. The number concentration range of the Ag particles was controlled to be 1000–2000 N cm⁻³. Although there are small fluctuations, the counting efficiency of the particles larger than 25 nm was nearly close to 100 % (T_s = 40°C), indicating that the loss of large particles or count missing of the OPC were negligible. These results proved that the OPC virtually counted all activated and grown particles which passed through its sensing zone. The reason why the OPC can count almost all the droplets is discussed in Answer 1.

We modified ‘Size-dependent particle counting efficiency’ part of the revised manuscript as following,

Figure 7 shows the size-dependent counting efficiency of the MEMS-based CPC. The size range of Ag particles was controlled concentration range to 1000-2000 N cm⁻³. The sampling times for each data point were 300 s, and the measurement uncertainty based on the Poisson statistics was 0.02%. To evaluate the effect of the temperature difference, the counting efficiency was characterized when the condenser temperature (T_c) was 10 °C and the saturator temperatures (T_s) were 30, 35 and 40 °C. At 40 °C (the design value of the saturator temperature), the same experiments were repeated three times to confirm the measurement reliability. When the saturator temperature was 40 °C, it was found that our system detected 1% of UFPs with the size of 5 nm, and the detection efficiency increased sharply above 9 nm. This was primarily because the activation efficiency (η_{act}) increased when the particle size exceeded the Kelvin diameter (2.34 nm). The transport efficiency (η_{trans}) also increased, because the diffusivity of a particle decreases with the increment of the particle size. The counting efficiency data were curve-fitted using

$$\eta_d = \alpha + \frac{(\beta - \alpha)}{1 + (d_p/\gamma)^\delta}, \quad (2)$$

where α , β , γ and δ are fitting constants of 101.96, 2.00, 12.99 and 4.70, respectively. The corresponding minimum detectable size is defined as the size at which particles are detected with 50% efficiency and was found to be 12.9 nm. The detection efficiency was 90% at 20.1 nm and reached 95% at 22.9 nm. It was close to 100 % and constant in the size range from 25 to 140 nm, indicating that the internal particle loss in this size range was negligible.

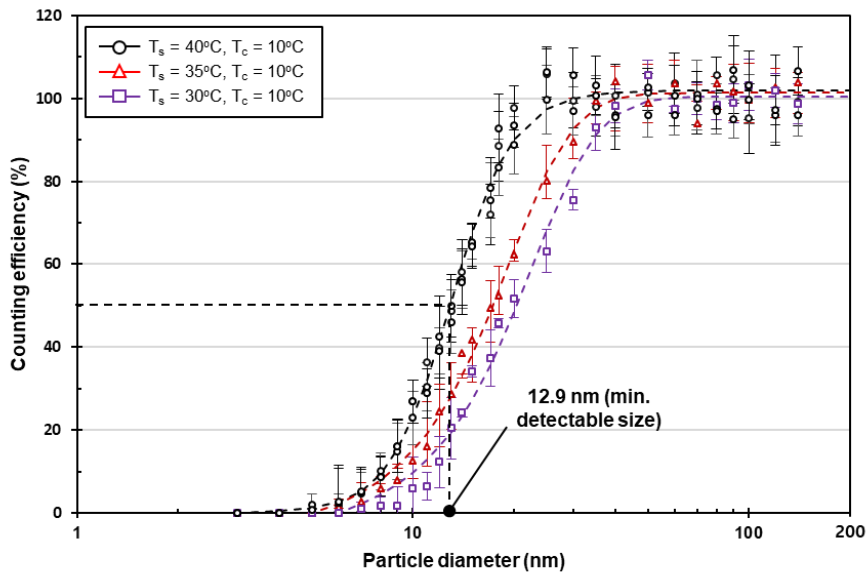


Figure 7: Particle counting efficiency of the MEMS-based CPC as a function of the particle size and saturator temperature. The particle size at which the particle counting efficiency was fitted to 50% was 12.9 nm (TS = 40oC), 17.3 (TS = 35) and 20.4 (TS = 30), respectively.

We added the procedures and assumptions for characterizing the counting efficiency in ‘Experimental setup’ part of the revised manuscript as following.

Because of the large difference between the flow rates of the reference instrument and our system, the following procedures were carried out to verify that particles with the same concentration were introduced into the two systems. First, to minimize system the particle loss induced from the turbulence at the bifurcation, a flow splitter with a very small angle of cleavage (model 3708, TSI Inc., USA) was used. The tubes which leads to the both systems were electrostatic dissipative to minimize the electrostatic particle loss, and their lengths were carefully adjusted to match the transportation times. To verify that the particles which introduced into both systems have the same concentrations, it was confirmed that the counting efficiency was close to 100 % when particles with size of 100 nm were introduced (it was assumed that they were activated and grew into droplets with 100 % efficiency). Then, while reducing the size of the introduced particles to 40 nm by adjusting the voltages of a DMA, it was confirmed whether the counting efficiency remained constant. Through these procedures, it was verified that the concentrations of the particles delivered to the two systems were the same. The loss of our system was characterized using the counting efficiency, since it is defined as the efficiency of the system at detecting the introduced particles, and thereby describes the overall transportation/activation efficiencies.

Question 14

P. 5, l. 28: The authors report on the detectable concentration range as measured with the temperature difference between the condenser and saturator set at 30 °C. Specify the conditions of operation of the CPC fully. The temperature difference between the saturator and the condenser are only part of the information that is needed. What was the saturator temperature? Of course, all temperature information is meaningless unless the authors specify their working fluid.

Answer 14

The temperatures of the saturator and condenser were 40 °C and 10 °C, respectively that we have written on page 2 of the original manuscript: “The saturated sample then enters a condenser, whose temperature (10 °C) is lower than that of the saturator (40 °C).”

Question 15

Fig 5 is very difficult to interpret as there is little contrast difference between the region where liquid is present and where the wick is dry. A bit of guidance as to how to interpret the picture is appropriate.

Answer 15

We modified the video frames in ‘Figure 5’ of the revised manuscript as following.

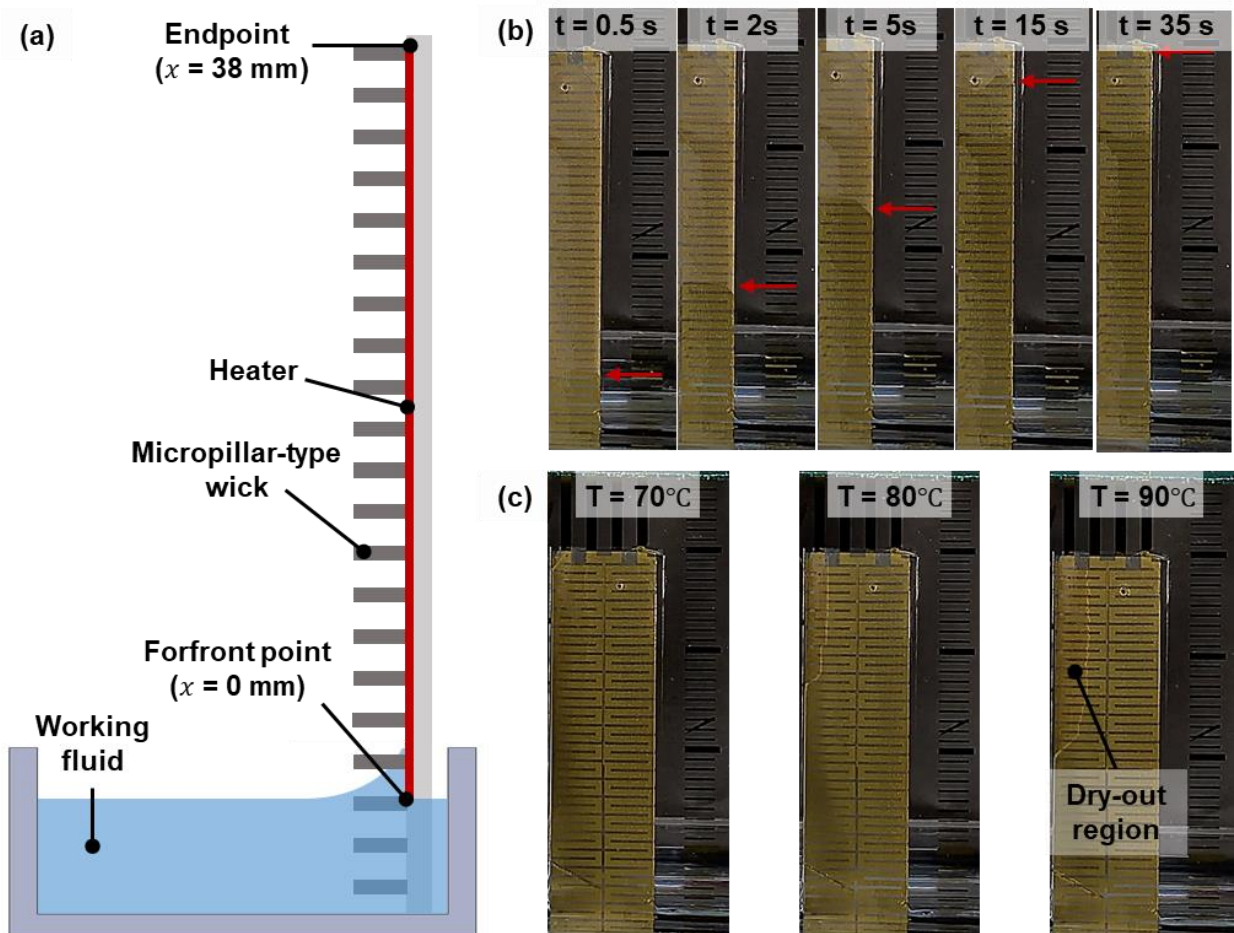


Figure 5: (a) Schematic of the capillary rise experimental setup; (b) selected video frames from the rise of the working fluid using micropillar-type wick; (c) the dry-out region formation as the surface temperature increased.

Question 16

Data are shown down to 3 nm which is not possible with the DMA that the authors report using. Did they use a different DMA for the sub-10 nm particles?

Answer 16

- 5 Thank for your correction. We used Ag particles in the size range from 3 to 140 nm. We classified the particles using two DMAs depending on their sizes: (1) nano DMA (model 3085, TSI Co. Ltd., USA) from 3 - 10 nm, (2) long DMA (model 3081A, TSI Co. Ltd., USA) from 11 - 140 nm.

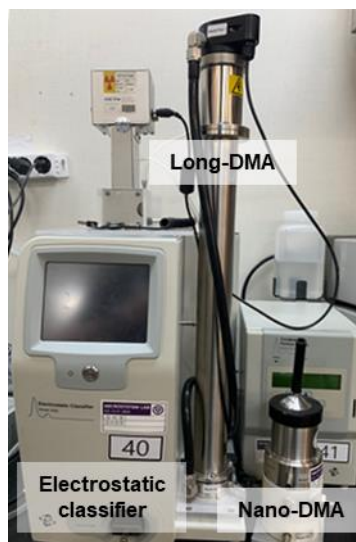


Figure R3: The (a) nano DMA and (b) long DMA used in this study.

10

We modified 'Experimental setup' part of the revised manuscript as following.

Figure 4 shows the experimental setup used to characterize the overall performance of the proposed system in terms of three aspects: (a) the clean air supply system, (b) monodisperse particle generating system, and (c) performance comparison system. Compressed air was used as the carrier gas. Any moisture, oil droplets, and particles in the compressed air were removed in the clean air supply system with an oil trap, diffusion dryer, and high-efficiency particulate (HEPA) filter. The purified air was then supplied to the particle generating system at a flow rate that was accurately controlled by a mass flow controller (MFC; VIC-D200, MKP Co., KR). Ag particles ranging in size from 3 nm to 140 nm were generated by an Ag particle generator (EP-NGS20, EcoPictures Co., KR). They were electrically charged by a soft X-ray charger (XRC-05, HCT Co., KR) and then classified to a specific diameter with two types of DMA: (1) nano DMA (model 3085, TSI Co. Ltd., USA) for particles in the size range from 3 to 10 nm, (2) long DMA (model 3081A, TSI Co. Ltd., USA) for particles in the size range from 5 to 140 nm. Next, the number concentration of the monodisperse Ag particles were controlled ($0-24000 \text{ N cm}^{-3}$) in the dilution bridge system by adjustment of the needle valve. Finally, the concentration-controlled and monodisperse Ag particles were introduced into our system and reference instrument, which was either a CPC (model 3772, TSI Inc., USA) or aerosol electrometer (model 3068B, TSI Inc., USA).

25

References

- Choi, K.-M., Kim, J.-H., Park, J.-H., Kim, K.-S., and Bae, G.-N.: Exposure characteristics of nanoparticles as process by-products for the semiconductor manufacturing industry, *Journal of occupational and environmental hygiene*, 12, D153-D160, 2015.
- 5 Donaldson, K., Li, X., and MacNee, W.: Ultrafine (nanometre) particle mediated lung injury, *Journal of Aerosol Science*, 29, 553-560, 1998.
- Donovan, R., Locke, B., Osburn, C., and Caviness, A.: Ultrafine aerosol particles in semiconductor cleanrooms, *Journal of The Electrochemical Society*, 132, 2730-2738, 1985.
- Hesterberg, T. W., Long, C. M., Bunn, W. B., Lapin, C. A., McClellan, R. O., and Valberg, P. A.: Health effects research and regulation of diesel exhaust: an historical overview focused on lung cancer risk, *Inhal Toxicol*, 24 Suppl 1, 1-45, 2012.
- 10 Hext, P.: Current perspectives on particulate induced pulmonary tumours, *Human & experimental toxicology*, 13, 700-715, 1994.
- Hristozov, D. and Malsch, I.: Hazards and risks of engineered nanoparticles for the environment and human health, *Sustainability*, 1, 1161-1194, 2009.
- 15 Kim, K. H., Sekiguchi, K., Kudo, S., and Sakamoto, K.: Characteristics of Atmospheric Elemental Carbon (Char and Soot) in Ultrafine and Fine Particles in a Roadside Environment, Japan, *Aerosol and Air Quality Research*, 11, 1-12, 2011.
- Kittelson, D. B.: Engines and nanoparticles: a review, *Journal of aerosol science*, 29, 575-588, 1998.
- Li, N., Georas, S., Alexis, N., Fritz, P., Xia, T., Williams, M. A., Horner, E., and Nel, A.: A work group report on ultrafine particles (American Academy of Allergy, Asthma & Immunology): Why ambient ultrafine and engineered nanoparticles should receive special attention for possible adverse health outcomes in human subjects, *J Allergy Clin Immunol*, 138, 386-396, 2016.
- 20 Li, N., Sioutas, C., Cho, A., Schmitz, D., Misra, C., Sempf, J., Wang, M., Oberley, T., Froines, J., and Nel, A.: Ultrafine particulate pollutants induce oxidative stress and mitochondrial damage, *Environmental health perspectives*, 111, 455-460, 2003.
- 25 Liao, B.-X., Tseng, N.-C., Li, Z., Liu, Y., Chen, J.-K., and Tsai, C.-J.: Exposure assessment of process by-product nanoparticles released during the preventive maintenance of semiconductor fabrication facilities, *Journal of Nanoparticle Research*, 20, 2018.
- Libman, S., Wilcox, D., and Zerfas, B.: Ultrapure Water for Advance Semiconductor Manufacturing: Challenges and Opportunities, *ECS Transactions*, 69, 17-28, 2015.
- Liu, L., Urch, B., Poon, R., Szyszkowicz, M., Speck, M., Gold, D. R., Wheeler, A. J., Scott, J. A., Brook, J. R., Thorne, P. S., and Silverman, F. S.: Effects of ambient coarse, fine, and ultrafine particles and their biological constituents on systemic biomarkers: a controlled human exposure study, *Environ Health Perspect*, 123, 534-540, 2015.
- 30 Manodori, L. and Benedetti, A.: Nanoparticles monitoring in workplaces devoted to nanotechnologies, 2009, 012001.
- Neisser, M. and Wurm, S.: ITRS lithography roadmap: 2015 challenges, *Advanced Optical Technologies*, 4, 235-240, 2015.
- Renwick, L., Brown, D., Clouter, A., and Donaldson, K.: Increased inflammation and altered macrophage chemotactic responses caused by two ultrafine particle types, *Occupational and Environmental Medicine*, 61, 442-447, 2004.
- 35 Shi, J. P., Khan, A., and Harrison, R. M.: Measurements of ultrafine particle concentration and size distribution in the urban atmosphere, *Science of the Total Environment*, 235, 51-64, 1999.
- Sousan, S., Koehler, K., Hallett, L., and Peters, T. M.: Evaluation of the Alphasense Optical Particle Counter (OPC-N2) and the Grimm Portable Aerosol Spectrometer (PAS-1.108), *Aerosol Sci Technol*, 50, 1352-1365, 2016.
- 40 Stolzenburg, M. R. and McMurry, P. H.: An ultrafine aerosol condensation nucleus counter, *Aerosol Science and Technology*, 14, 48-65, 1991.